Supporting Information

Shortening the Reaction Pathway of Sulfur Redox Kinetics with 2,5-Dichloro-1,4-Benzoquinone to Minimize the Shuttle Effect in Lithium-Sulfur Batteries

Jiayi Shao[a], Hanxiao Wang[b], Xinjie Huang[a], Xianguo Ma[c], Xuyun Wang[a], Hongsheng Huang[c], Jianwei Ren [d,*], Rongfang Wang[a,*]

[a] College of Chemical Engineering, Qingdao University of Science and Technology, Qingdao, 266042, China

[b] Qingdao Institute of Bioenergy and Bioprocess Technology, Chinese Academy of Sciences, Shandong Energy Institute, Qingdao New Energy Shandong Laboratory, Qingdao 266101, China

[c] School of Chemical Engineering, Guizhou Institute of Technology, Guiyang 550003, China

[d] Department of Chemical Engineering, University of Pretoria, cnr Lynnwood Road and Roper Street, Hatfield 0028, South Africa.

*Corresponding author.

E-mail address: jianwei.ren@up.ac.za (J. Ren);
rfwang@qust.edu.cn (R.Wang)

1. Assembly and Testing of Lithium-Sulfur (Li-S) Batteries

A mixture of S@Fe-NC (70 wt. %), Super P conductive carbon black (20 wt%), and binder PVDF (10 wt.%) was dissolved in N-methyl-2-pyrrolidone (NMP). The resultant slurry was then coated onto an aluminum foil current collector. The electrodes were

vacuum-dried at 60 °C for 12 h to remove the solvent. The dried electrodes were then cut into discs with a diameter of 12 mm. The typical sulfur loading in the electrode was 1.3–1.9 mg cm^{-2}. Celgard 2400 was used as the separator, and lithium metal was used as the anode. CR2032-type stainless steel coin cells were assembled in an argon-filled glove box.

For electrochemical performance testing, the current density settings and specific capacity calculations were referenced to the sulfur mass in the cathode (1 C = 1675 mAh g^{-1}). The cells were tested on a Newave battery system within a voltage range of 1.7–2.8 V. Cyclic voltammetry (CV) and electrochemical impedance spectroscopy (EIS) were performed using a CHI 650D electrochemical analyzer. The CV tests were conducted at scan rates and voltage ranges of 0.1–0.5 mV s^{-1} and 1.7–2.8 V, respectively. EIS measurements were conducted in the frequency range of 100 kHz to 10 mHz. All electrochemical tests were performed at room temperature. To calculate the Li^+ diffusion coefficient, the ionic diffusion resistance in the EIS data was fitted, and the following formulas (1) and (2) were used for the calculation:

$$Z_{real} = R_e + R_{ct} + \sigma\omega^{-1/2} \quad \textbf{(S1)}$$

$$D = \frac{R^2T^2}{2A^2n^4F^4c^2\sigma^2} \quad \textbf{(S2)}$$

In the formulas, the variables are defined as follows: **R**–Gas constant; **T**–Absolute temperature; **A**–Electrode area; **n**–Number of electrons transferred; **F**–Faraday constant; **c**–Li^+ concentration and **σ**–Weber factor.

2. Li_2S Nucleation Experiment

CR2032 button cells were assembled using S@Fe-NC electrodes for the working electrode, lithium metal for the anode, and Celgard 2400 as the separator. A 20 μL solution of 0.2 M Li_2S_8 in tetraethylene glycol (TEG) electrolyte was added to the working electrode side. Simultaneously, 20 μL of electrolyte without Li_2S_8 was added

to the anode side. To study the Li_2S nucleation kinetics, the assembled cells were discharged at a constant current of 0.112 mA until the voltage dropped to 2.06 V, then held at a constant voltage of 2.05 V until the current decreased to below 0.01 mA to ensure the complete nucleation of Li_2S.

3. **Physical Characterization**

The materials and solvents used in this study were purchased from commercial sources (e.g., Aldrich, Canrd, Dodochem) and did not require further purification. Scanning electron microscopy (SEM) was performed using a Carl Zeiss Ultra Plus microscope from Germany. X-ray photoelectron spectroscopy (XPS) analysis was conducted using a British VG Escalab 210 instrument with an Mg 300-W X-ray source.

4. **Theoretical Calculations**

The density functional theory (DFT) method with the B3LYP functional was applied using the 6-311G(D) basis set in the Gaussian 09 program, with the empirical keyword (em=gd3bj) in Gaussian 09. All structures were optimized and validated without any imaginary frequencies. The lowest unoccupied molecular orbital (LUMO) and highest occupied molecular orbital (HOMO), as well as the electrostatic surface potential (ESP), were plotted and visualized using Multiwfn and Visual Molecular Dynamics (VMD). The thermodynamic values of Gibbs free energy were calculated using Shermo. Intra-molecular interactions were calculated using the reduced density gradient function (RDG), referred to as RDG in the text.

5. **Results**

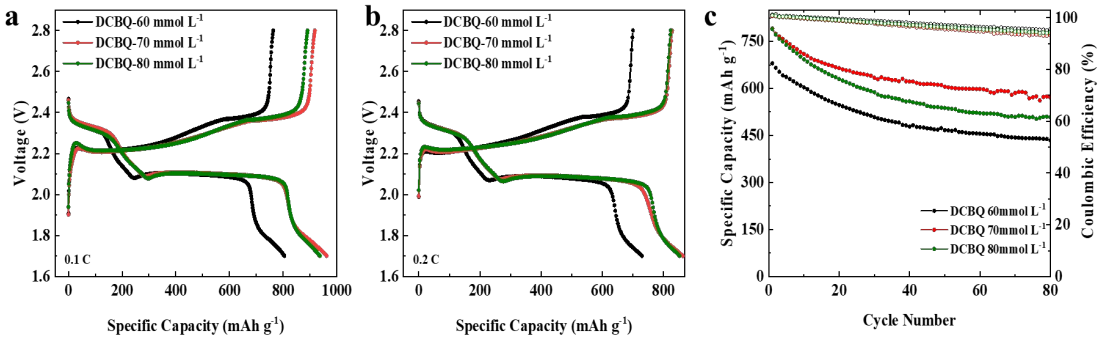

Figure S1. Charge-discharge curves of DCBQ at concentrations of 60, 70, and 80 mmol L^{-1} at (a) 0.1 C and (b) 0.2 C, and (c) long-cycle performance at 0.2 C.

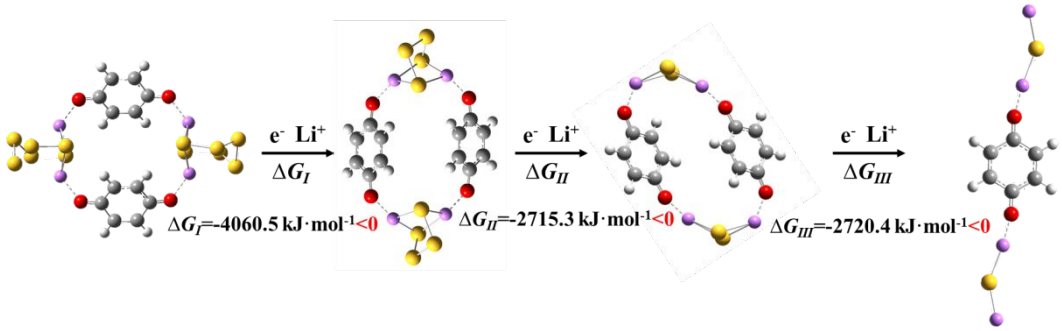

Figure S2. Bond-breaking mechanisms of 2PBQ-2Li_2S_6 during the discharge process and the Gibbs free energy at each step.

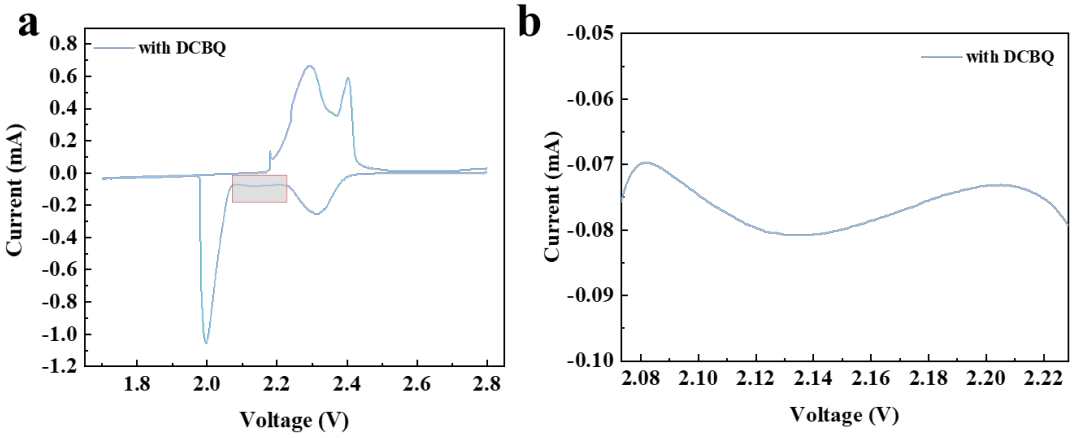

Figure S3. (a) Cyclic voltammetry (CV) curves of the battery with DCBQ additive at a scan rate of 0.05 mV s^{-1}, and (b) zoomed-in view of the region between 2.07–2.23 V.

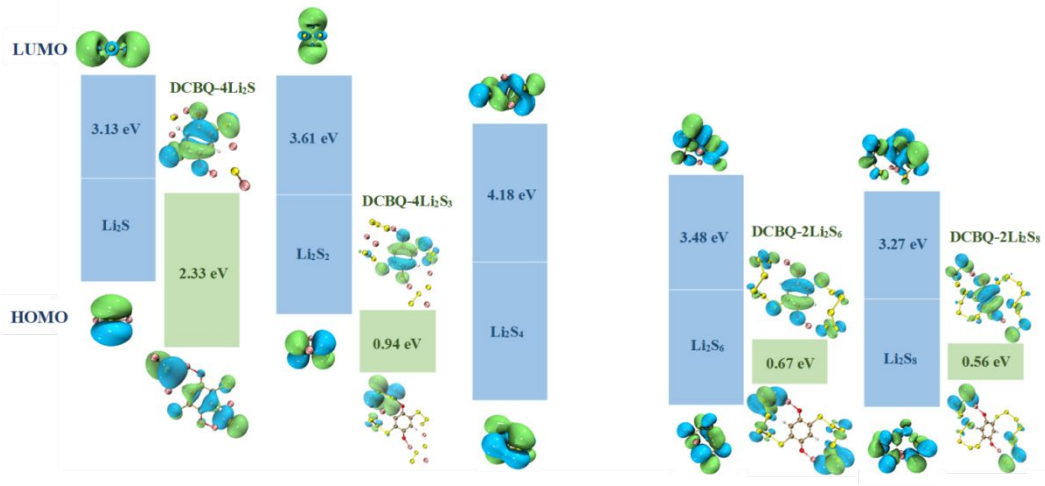

Figure S4. Frontier molecular orbital (FMO) energy levels of Li_2S_x and DCBQ-Li_2S_x.

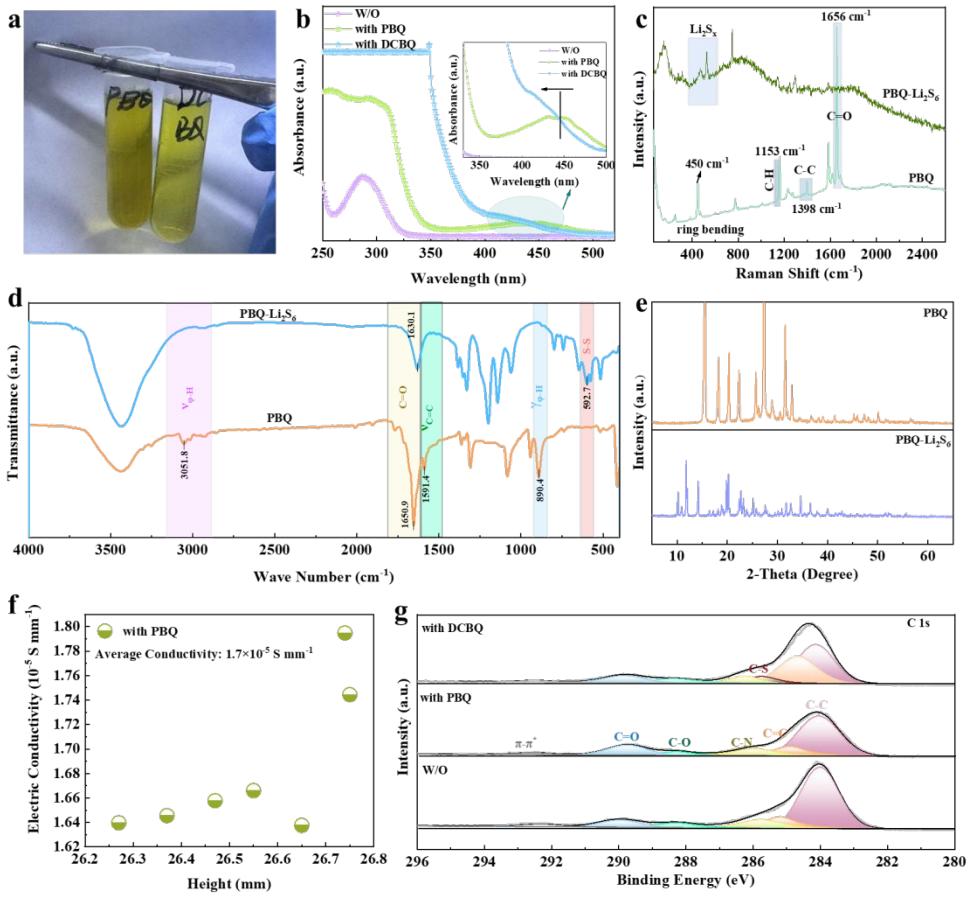

Figure S5. (a) Visualization of the colors of two electrolyte additives; (b) UV-Vis spectra of blank electrolyte, PBQ, and DCBQ samples; (c) Raman spectra of PBQ and PBQ-Li_2S_6; (d) Infrared spectra of PBQ and PBQ-Li_2S_6; (e) XRD spectra of PBQ and PBQ-Li_2S_6; (f) Conductivity curve of PBQ-Li_2S_6 intermediate; (g) High-resolution C 1s XPS spectra of the S cathode in Li-S batteries after 50 cycles at 0.2 C.

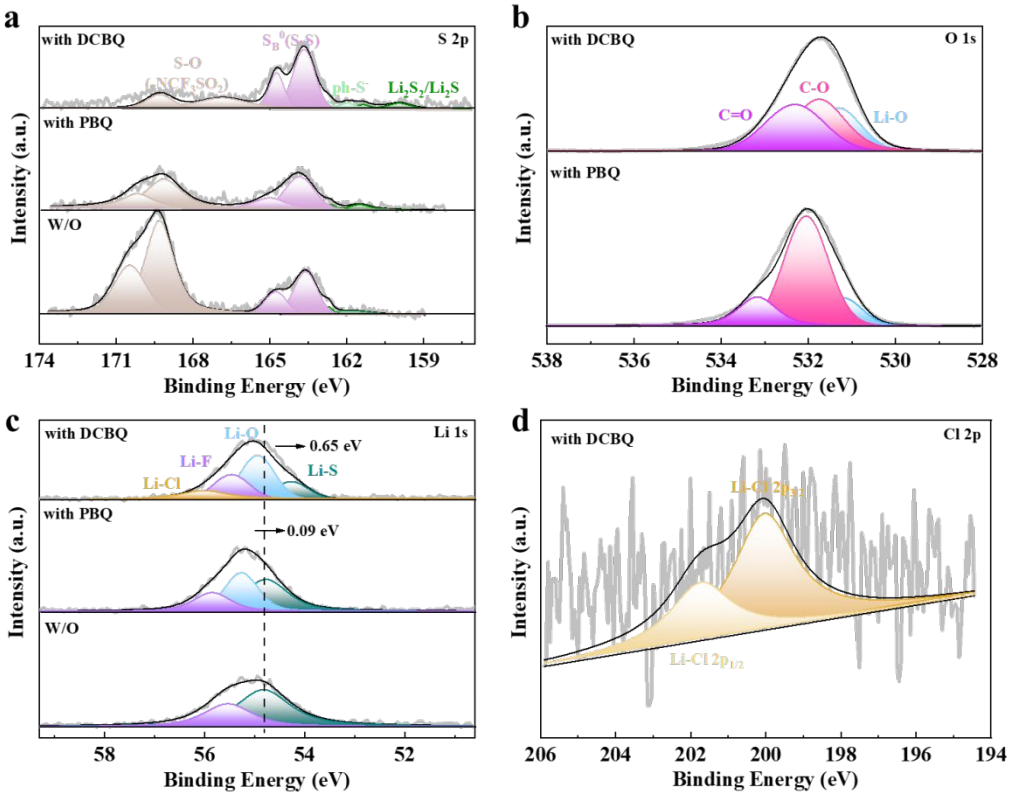

Figure S6. XPS spectra of the lithium anode surface in Li-S batteries after 50 cycles at 0.2 C for four samples: (a) S 2p, (b) O 1s, (c) Li 1s, and (d) Cl 2p.

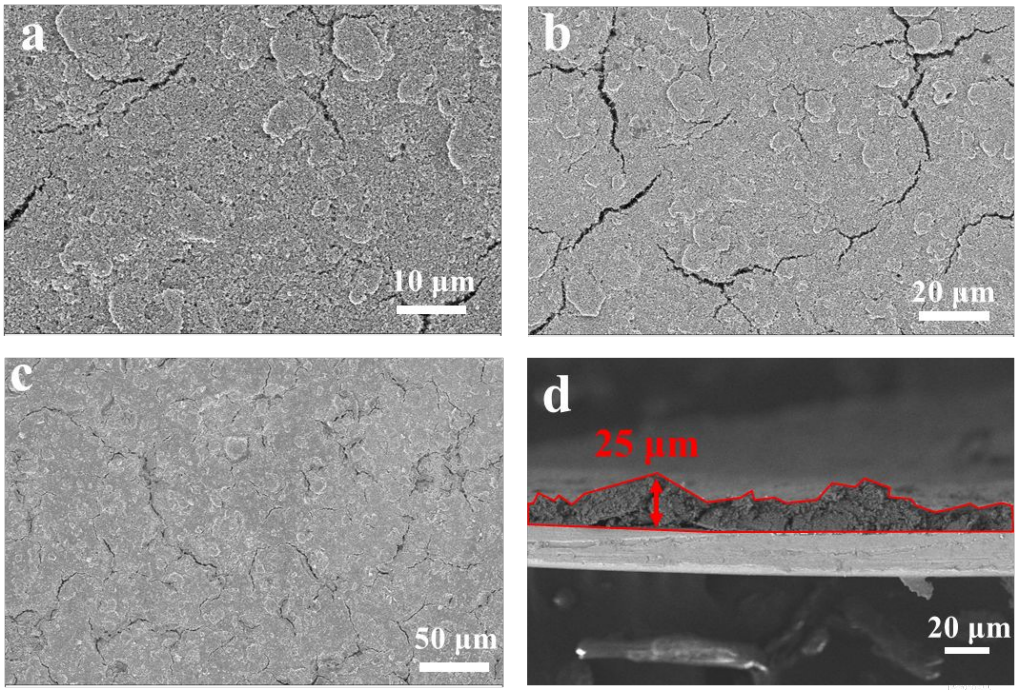

Figure S7. Top view images of the sulfur cathode in the PBQ battery after 50 cycles: (a) at 10 μm, (b) at 20 μm, and (c) at 50 μm, and (d) side view image at 20 μm.

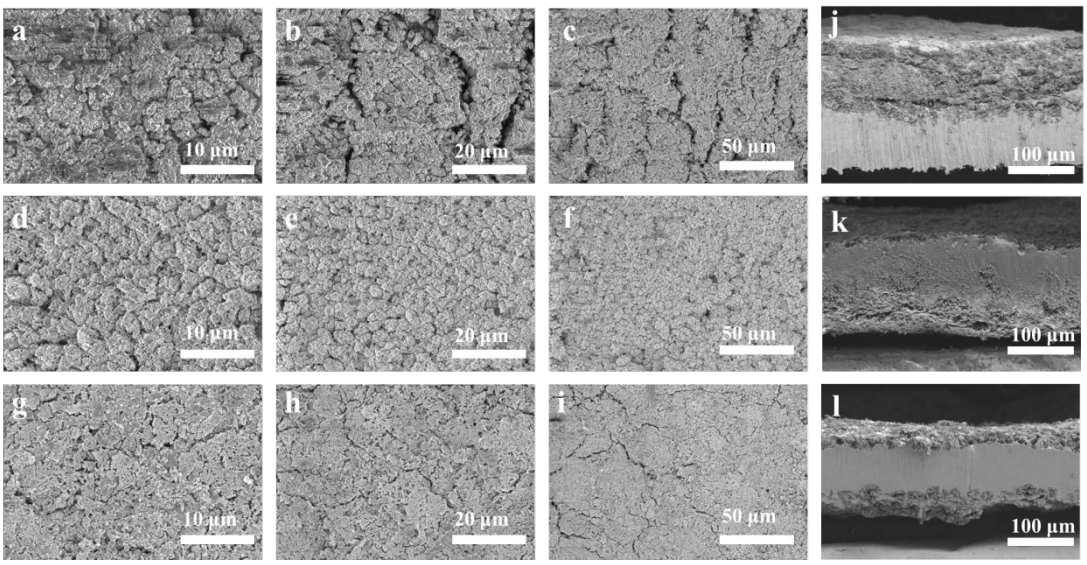

Figure S8. Vertical view of the lithium anode in the Li-Li symmetric cells with (a–c) blank electrolyte after 50 cycles at different magnifications, (d–f) PBQ, and (g–i) DCBQ. Side view of the lithium anode in the Li-Li symmetric cells after 50 cycles for (j) W/O, (k) PBQ, and (l) DCBQ.

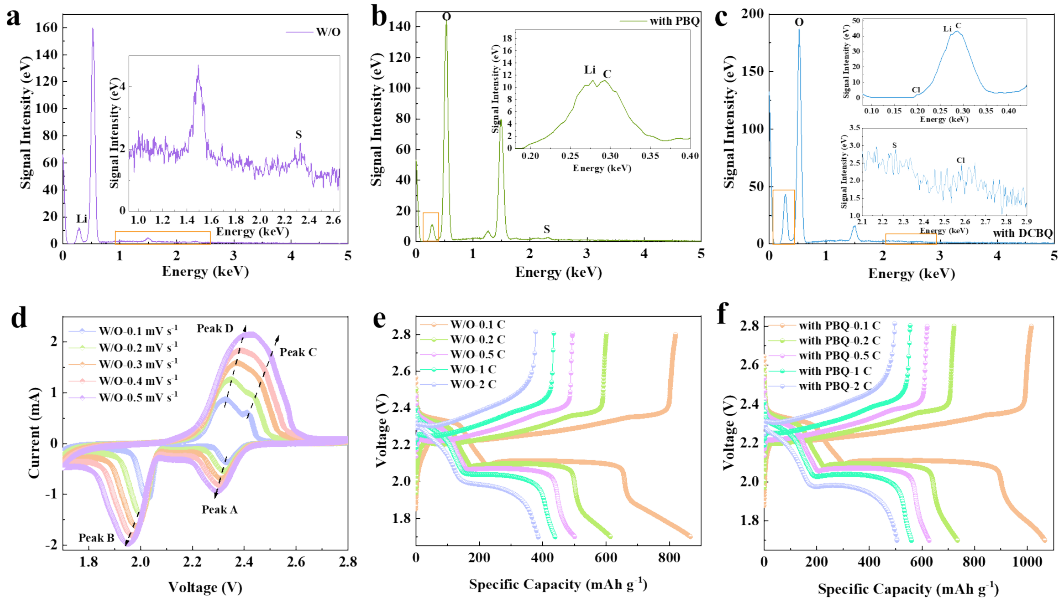

Figure S9. EDS spectra of the lithium anode interface for three types of batteries: (a) blank control group, (b) with PBQ, and (c) with DCBQ. (d) CV curves of the blank electrolyte sample at different scan rates, (e) Charge-discharge curves of the blank electrolyte sample, and (f) PBQ sample at different current densities.

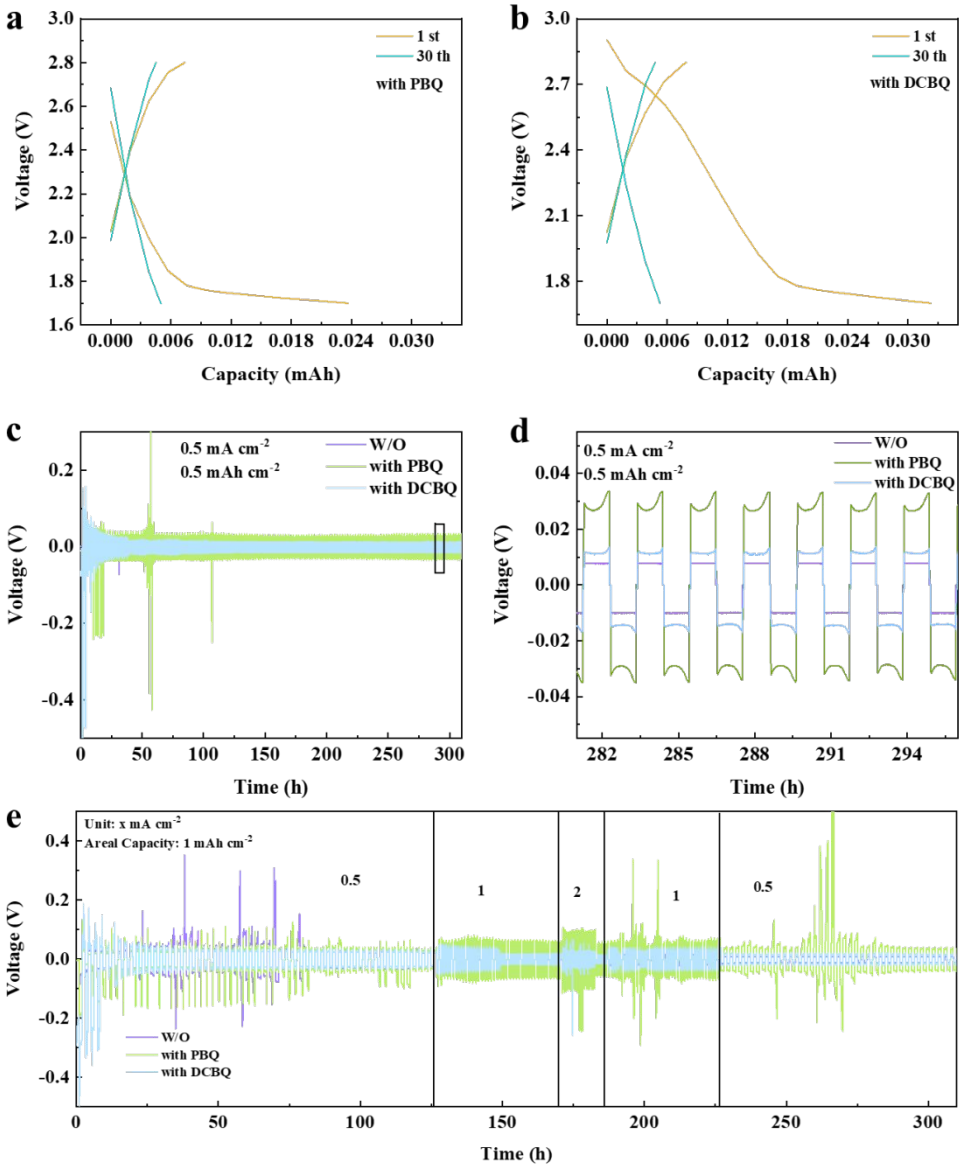

Figure S10. (a) Charge-discharge curves of sulfur-free (a) Li-PBQ and (b) Li-DCBQ batteries in the first and 30th cycles at a current density of 0.2 mA cm^{-2}. (c) Cycle stability. (d) Enlarged image of the lithium-lithium symmetrical cell at a current density of 0.5 mA cm^{-2}. (e) Rate performance of the Li||Li symmetric battery.

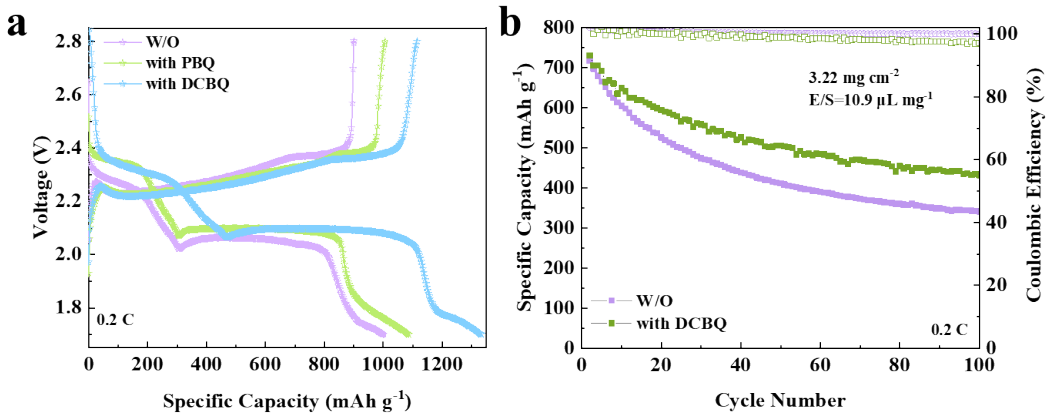

Figure S11. (a) First cycle charge-discharge curves of W/O, PBQ, and DCBQ at 0.2 C. (b) Cycle stability curve of the battery in high sulfur loading and lean electrolyte conditions.

Table S1 Gibbs free energy of each substance.

	PBQ	DCBQ	Li_2S_6	PBQ- Li_2S_6	DCBQ- Li_2S_6	LiCl
G (Hartree)	-381.406	-1300.607	-2404.397	-5571.635	-5173.762	-467.848

Table S2. Li^+ diffusion coefficients at different peak positions.

D_{Li^+} ($cm^2\ s^{-1}$)	A (cathodic peak)	B (cathodic peak)	C (cathodic peak)	D (cathodic peak)
W/O	$2.93*10^{-7}$	$6.76*10^{-7}$	$1.1*10^{-6}$	$1.37*10^{-6}$
with DCBQ	$1.28*10^{-6}$	$2.98*10^{-6}$	$3.43*10^{-6}$	$2.49*10^{-6}$

$$I_p = (2.69 \times 10^5 \times n \times A \times {D_{Li}}^{0.5} \times C_{Li} \times v^{0.5}) \quad \textbf{(S3)}$$

$\boldsymbol{I_p}$**:** Peak current (A)

$\boldsymbol{n}$: The number of electrons involved in the reaction (n=2)

$\boldsymbol{A}$: The electrode area (A=1.13 cm^2)

$\boldsymbol{D_{Li}}$: The diffusion coefficient of Li^+

C_{Li}: The concentration of Li^+ in the electrolyte

v: The scan rates.

Table S3. Li^+ Conductivity

	W/O	with PBQ	with DCBQ
D (cm^2 S^{-1})	$4.3*10^{-13}$	$6.55*10^{-12}$	$6.63*10^{-11}$

$$D = \frac{R^2T^2}{2A^2n^4F^4c^2\sigma^2} \quad \textbf{(S4)}$$

R: Gas constant (8.314 J/mol·K)

T: Absolute temperature (Kelvin)

A: Electrode area (cm^2)

n: Number of electrons transferred (usually 2 for lithium-ion reactions)

F: Faraday constant (96485 C mol^{-1})

c: Li^+ concentration (mol/cm^3)

σ: Weber factor (dimensionless)